

ACCURACY OF TWO CBCT SOFTWARE USING SEMI-AUTOMATED SEGMENTATION OF SIMULATED BONE DEFECTS

Yasmein Maher El-Beblawy* , Maha Ishaq Amer** 
and Ahmed Mohamed Bakry*** 

ABSTRACT

Purpose: The aim of this study was to evaluate the accuracy and reliability of simulated osteolytic jaw lesions' volumes measured on 2 CBCT software using semiautomated segmentation.

Materials and methods: 8 simulated bone defects were created at the cancellous bone of 2 human cadaveric mandibles. A replica was prepared to represent the actual size of the created defects. Then screening radiographs were taken for these defects with 10 mA and 90 kV, FOV 50 X 100 mm, 3 seconds of effective exposure time, and focal spot 0.5 mm. 2 software were used to perform segmentation OnDemand and Mimics which were adaptable to the processing system.

Results: Linear regression models for studied methods in estimating impression volume were calculated. Pair-wise comparisons revealed no statistically significant difference between Mimics and OnDemand software.

Conclusion: A semiautomated method for CBCT images has several advantages over manual analysis; the risk of nonobjectivity and interobserver variability is greatly reduced by minimizing the active manual input of the user. Thus, Mimics is more reliable and accurate than OnDemand.

KEY WORDS: Odontogenic Cyst; Cyst Volume; Segmentation; Volume Analysis; CBCT.

INTRODUCTION

The utilization of radiological image data is steadily increasing in various therapeutic fields, resulting in a continuous and rapid rise in the importance of image-based segmentation and

three-dimensional image analysis. The subject of picture segmentation holds significant prominence in the realm of image processing. Segmentation is the act of partitioning an image into discrete and mutually exclusive regions of pixels, utilizing

* MD , Minia

** Professor, Oral Maxillofacial Radiology Department, Faculty of Dentistry, Minia University, Minia, Egypt.

*** Assistant Professor, Oral and Maxillofacial Radiology Faculty Of Dentistry Minia Univeristy

various criteria such as grayscale values, color attributes, spatial texture, and geometric shapes. The procedure entails dividing the image into multiple segments through the identification and analysis of similarities or dissimilarities across these sections. Image segmentation is a crucial procedure in diverse biomedical-imaging applications, which includes tasks such as quantifying tissue volumes, diagnosing diseases, detecting pathological regions, analyzing anatomical structures, devising treatment plans, and integrating computer-assisted surgical procedures (**Kumar et al., 2018; Wallner et al., 2019; Ramesh et al., 2021**).

A unique grayscale value is assigned to each voxel, which corresponds to the quantity of radiation it absorbs. In the course of three-dimensional reconstruction, the mean grayscale intensity of a voxel is calculated when it encompasses tissues exhibiting diverse densities. The application of quantitative analysis using grayscale values obtained from cone-beam computed tomography (CBCT) imaging is constrained by the process of voxel averaging. The process of medical image segmentation can be classified into the following stages: Obtain a medical imaging dataset that conventionally consists of a training set, a validation set, and a test set. In the domain of utilizing machine learning methodologies for image processing, it is customary to divide the dataset into three separate groups. In this particular context, the training set is utilized to assist the process of training the network model. The verification set is employed to fine-tune the hyperparameters of the model. Lastly, the test set is used to evaluate and confirm the final performance of the model (**Shaheen E et al., 2017 and Liu, X et al., 2021**).

The image undergoes preprocessing and augmentation through various procedures, including the standardization of the original image and the application of random rotation and scaling. These techniques are utilized to enhance the dataset by expanding its magnitude. Employ an appropriate

medical image segmentation methodology to divide the medical image, hence producing the segmented images. An assessment of the accuracy and effectiveness of estimation performance. In order to evaluate the effectiveness of medical image segmentation, it is crucial to create suitable performance metrics for the purpose of verification. This particular component constitutes an essential element of the aforementioned technique (**Shaheen et al., 2017 and Liu et al., 2021**).

The classification of image segmentation techniques includes manual, automatic, and semi-automatic methods. One of the segmentation approaches employed is manual segmentation, which involves the user manually outlining the structure of interest on each slice of a 3D image by marking voxels. In order to undertake this activity, it is necessary to have prior knowledge pertaining to the particular shape of the building being examined, as well as an understanding of the intensity of grey values that compose its related image. The technique discussed above demonstrates a notable degree of accuracy. However, its effectiveness relies on the user and necessitates a substantial time investment, making it applicable mostly to image datasets that are relatively small in scale. The importance of employing manual segmentation is in its ability to provide precisely labeled images, which serve as the basis for the development of semi-automatic and fully automatic segmentation methods (**Haque et al., 2020**).

Semi-automatic segmentation methodologies, alternatively referred to as interactive segmentation techniques, utilize a combination of user input and automated procedures. This methodology combines the effectiveness of automated operations with the accuracy of hand segmentation conducted by experts in the field. The method of user engagement involves the initial selection of an estimated return on investment (ROI), which is subsequently used to segment the entire image. The procedure may involve the manual scrutiny and

modification of territorial boundaries in order to alleviate segmentation mistakes. Numerous semi-automatic segmentation strategies have been put forth in the academic literature. The methodologies encompassed in this study are the seeded region growth (SRG) algorithm, the level-set-based active contour model, and the localized region-based active contour techniques (**Gomes AF et al., 2020**).

The primary aim of this research was to evaluate the accuracy and reliability of two cone beam computed tomography (CBCT) software systems in quantifying the volumes of artificially created bone defects.

MATERIALS AND METHODS

The study received ethical permission from the Research Ethics Committee (REC) of the Faculty of Dentistry, Minia University, with the assigned approval number 534 – 1/11/2021.

A total of eight osteolytic lesions were artificially created in the cancellous bone of 2 dry human mandibles, provided by the Department of Anatomy, Faculty of Medicine, Minia University, using dental burs, in order to replicate bone lesions of varying sizes and shapes. In order to replicate the reduction in signal strength induced by soft tissue in an in vivo setting, wax sheets (specifically, Base Plate Wax Cavex and Modelling Wax from the Netherlands) measuring 175 mm in length, 80 mm in width, and 1.5 mm in thickness were employed. The sheets were arranged in a sequential manner, with each subsequent sheet positioned beneath the previous one and numbered in ascending order. Care was taken to ensure that the sheets were pressed together gently, minimizing any gaps between them, while also ensuring that the wax material was not distorted. To accurately measure the volume of the lesions, the volume of each bone defect was assessed by taking an impression using Rapid soft silicone (Vinylight) impression material. Subsequently, the volume was estimated using the water displacement technique.

The artificial bone replicas were assessed by measuring their weight using an electronic analytical balance (Shimadzu Corporation Aty224, Kyoto, Japan) with a precision of 0.0001 grams. The measured weight of the material was documented. The electronic balance utilized in this study incorporated a comprehensive automated calibration system and a highly precise micro-weighing scale, enabling the correct measurement of values for all samples. Prior to weighing, every mounted sample was meticulously cleaned and thoroughly dried using tissue paper. In order to maintain precision, the balance was consistently placed on a stable table, isolated from any vibrations. The specimens were weighed with the glass doors of the balance securely shut, therefore mitigating the influence of air. The weight of each imprint sample was divided by the known density of Rapid soft silicone (Vinylight) 1.40 gm/cm³ to determine the average weight. The volume of each of the impression samples was determined using the calculation, as reported by **O'Brien W.J. in 2002** and **Ahlowalia MS et al. in 2013**.

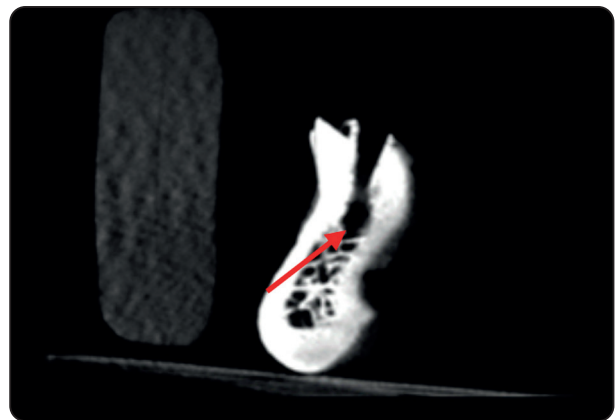


Fig. (1) Dry mandibles. B. CBCT images after preparation of simulated defects (red arrow)

Screening radiographs and CBCT scans were taken for the dry mandibles with the simulated defects. The examinations were carried out using a standardized method to ensure the reproducibility of the examination and the reliability of the analysis of the artificial defects was used. CBCT examinations of the simulated pathosis were performed using

(SCANORA® 3Dx, Soredex, Tuusula, Finland) with 10 mA and 90 kV, FOV 50 X 100 mm, 3 seconds of effective exposure time, and focal spot 0.5 mm.

Volumetric analysis

Mimics and OnDemand software were used for volume detection of the simulated bone defects according to each manufacturer's recommendations using interactive thresholding with manual refining. The data was collected and reported in a chart. The volume of the replica represented the physical volume (V_p) of the prepared bone defects.

Statistical Analysis

Numerical data were explored for normality by checking the distribution of data and using tests of normality (Kolmogorov-Smirnov and Shapiro-Wilk tests). All data showed non-normal (non-parametric) distribution. Data were presented as range, mean, and standard deviation (SD) values.

TABLE (1) Showed that: Descriptive statistics of the studied volumes, Mean \pm SD of OnDemand and Mimics were 393.6 \pm 122.0 and 396.1 \pm 127.3 respectively.

Method	Mean \pm SD	Range
OnDemand (mm ³)	393.6 \pm 122.0	242.2–535.3
Mimics (mm ³)	396.1 \pm 127.3	239.9–533.2

Total=8

TABLE (2) Interclass correlation (ICC) between impression volume and the studied methods and their corrected in estimating impression volume

Method	Chronbach's α	95% CI	p-value#	p-value^
OnDemand	0.993	0.963–0.999	<0.001*	0.999
Mimics	0.997	0.986–0.999	<0.001*	
Corrected OnDemand	0.993	0.966–0.999	<0.001*	
Corrected Mimics	0.997	0.983–0.999	<0.001*	

Total=8. CI: Confidence interval. #p-value between each software. ^p-value between the studied software.

Table showed that Mimics and corrected Mimics had the highest significant interclass correlation with Impression volume, followed by OnDemand and corrected OnDemand.

The inter-examiner agreement was assessed using Cronbach's alpha reliability coefficient and Intra-Class Correlation Coefficient (ICC). Closer values of these coefficients to one indicate better inter-observer agreement. Qualitative data were presented as frequencies and percentages. The significance level was set at $P \leq 0.05$. Statistical analysis was performed with IBM SPSS Statistics for Windows, Version 23.0. Armonk, NY: IBM Corp.

RESULTS

The present study was conducted on 8 CBCT scans of simulated well-defined osteolytic lesions. Pair-wise comparisons revealed no statistically significant difference between Mimics and OnDemand software.

The table showed that OnDemand and MIMICS had the smallest and narrowest deviation from impression volume, followed by corrected OnDemand and corrected Mimics.

TABLE (3) Deviations of the studied software and their corrected in estimating measures from impression volume

Methods	Median	1 st –3 rd IQ	IQ range	Min.–Max.	Range
OnDemand	-25.9	-49.0–23.2	25.8	-52.7–14.7	67.4
Mimics	-24.8	-32.6–14.3	18.3	-55.0–12.4	42.6
Corrected OnDemand	-7.3	-15.4–8.0	23.4	-15.9–46.5	62.4
Corrected Mimics	-8.7	-11.6–16.2	27.8	-22.2–20.0	42.2
p-value Δ			<0.001*		

*Total=8. IQ: Interquartile. Δ Friedman test. *Significant*

DISCUSSION

The choice of MIMICS was made due to its widespread application in the field of Biomedical engineering. The MIMICS program provides a semiautomated feature. The software referred to as OnDemand is installed and utilized on a workstation situated inside a designated geographic region. The OnDemand 3D software program has several significant advantages, such as its intuitive user interface and strong capability to import a large quantity of DICOM files, enabling the creation of high-quality three-dimensional images. However, the proprietary nature of the software poses a significant limitation that may impede its implementation in diverse academic institutions.

The segmentation procedure employed in this study adhered to the parameters stated by the respective software manufacturers. Furthermore, the study utilized the interactive threshold technique, in which the operator manually calculated the best threshold range for precisely visualizing the whole anatomical borders of the simulated lesions. Variation in the threshold level was detected among the various software programs. It can be argued that the interactive threshold technique is susceptible to the impact of human capabilities, perhaps resulting in an overestimation or underestimation of the actual magnitude of the lesion.

Higher deviation was found in Ondemand software than MIMICS this can be imputed to the use of the interpolation tool which causes improper segmentation of some slices; therefore, 3D visualization will show irregularity of the volume constructed in the 3D viewer. In this study, upon noticing this mistake, it was remedied by rectifying and refining the segmentation (on the slice affect. MIMICS and OnDemand; both showed statistically significantly greater deviation error in dry mandible volumetric measurements than the volume of the replica (gold standard) (Fadili A et al., 2018).

A semi-automated method, represented in this study by OnDemand and MIMICS software, has several advantages; the risk of nonobjectivity and interobserver variability is greatly reduced by minimizing the active manual input of the user. The semi-automated approach can be purely objective and handle every dataset in exactly the same manner. Thus, by the semiautomated method, the analysis of the larger number of scans can be evaluated compared to manual segmentation. To enable the researcher to check every step along the way, the semiautomated method generates visualizations of the segmented volume. These visualizations can be evaluated after the analysis is complete (Fadili A et al., 2018).

This can also be attributed to the segmentation method by using a scalpel for trimming the areas that do not belong to the segmented lesion. This is

in rapport with **Weissheimer et al 2012** who used a known acrylic phantom volume as a gold standard to compare the accuracy of software programs including MIMICS and OnDemand for measuring the upper airway volume. Their results showed that OnDemand had a higher percentage of errors than the rest of the software programs (including MIMICS) when compared with the gold standard. **Park CW et al., 2017** showed good overall performance of OnDemand software, allowing the segmentation and volume measurements of Four geometric phantom objects.

Manual editing may result in over or under-segmentation by the observer. Semi-automatic segmentation refers to the process, whereby this automatic segmentation is followed by manual checking and editing of the segment boundaries. Semi-automatic segmentation also requires more time as it involves manual checking and editing, which involves many slices of two-dimensional data. This time factor is the main drawback of semi-automatic segmentation in the routine clinical setting, let alone the steep learning curve to learn how to use that particular software.

This discovery is consistent with the research conducted by **Vallaey's et al. (2015)**, which determined that effectively segmenting periradicular cysts is difficult due to their variable characteristics and the frequent absence of a clear grey gradient near their margins. As a result, the semi-automatic approach frequently leads to an over-expansion of the segmentation, surpassing the targeted borders of the cyst. The lack of distinct features that can clearly define the boundaries of the lesions presents a significant barrier to achieving precise segmentation. This phenomenon gives rise to the possibility of either underestimating or overestimating the magnitude. The task of accurately segmenting objects becomes difficult when the visual characteristics, such as boundaries and regions, do not possess sufficient density, robustness, or discriminative skills. This challenge

persists even when manual processes are utilized. Each strategy requires a certain degree of sacrifice.

The study undertaken by **Stoetzer M et al. (2013)** aimed to assess the effectiveness of a threshold-based algorithm in the evaluation of cyst volume. The researchers arrived at the conclusion that this particular approach did not produce consistent results. Within the field of medicine, it seems unfeasible for a segmentation algorithm to meet all the requisite criteria owing to the considerable disparities in characteristics observed among organs and tissues (**Yau HT et al., 2014**). To address these concerns, the segmentation process requires a thorough comprehension of the images being analyzed and the precise data that has to be retrieved. A thorough comprehension of the conditions enables individuals to differentiate between superfluous elements and important knowledge.

The presence of intrinsic subjectivity in this particular methodology has the potential to yield divergent outcomes between two users or even within a single user when comparing two segmentations of the same tooth (**Vallaey's K et al., 2015**). The comparative dependability of an interactive threshold is diminished when contrasted with a set threshold, as the latter obviates the possibility of operator subjectivity in the determination of boundaries. To obtain a comprehensive evaluation of software performance, it is crucial to analyze the intrinsic differences between CT and CBCT in relation to the assessment of density units, while considering the use of these two threshold selection systems. The Hounsfield Unit (HU) in computed tomography (CT) scans has a direct correlation with the degree of x-ray attenuation. Each pixel is assigned a value to graphically represent the density of tissue within the image. Cone-beam computed tomography (CBCT) use grayscale representations, specifically voxel values, to illustrate the degree of x-ray attenuation. The voxel values are represented in Hounsfield Units (HU). Nevertheless, it is crucial to acknowledge that the Hounsfield Unit (HU) measurements obtained from Cone Beam Computed

Tomography (CBCT) scans are not inherently precise representations. Instead, they undergo necessary changes during a post-processing stage to ensure alignment with the grey scale.

Furthermore, disparities in cone-beam computed tomography (CBCT) scanner might lead to divergences. Hence, the adoption of a predetermined threshold based on Hounsfield Units (HU) is deemed to be the most effective approach for assessing the performance of software in the context of computed tomography (CT) images. The application of a predetermined threshold in the evaluation of cone-beam computed tomography (CBCT) images may generate a potential bias when comparing different software algorithms in their capacity to precisely detect, align, and complete specified areas. The aforementioned bias is especially evident in situations when there are complex morphological characteristics and/or little differentiation between visual elements. The aforementioned phenomenon has been documented in research undertaken by Weissheimer et al. (2012) and Lo Giudice et al. (2022).

ACKNOWLEDGMENT

I convey my sincere gratitude to my supervisors for their kind and proper guidance in every phase of the project.

REFERENCES

1. Fadili A, Halimi A, Benyahia H, Zaoui F. Stereology volume analysis to evaluate teeth's root using CBCT images. *Reports in Medical Imaging Volume*. 2018; 11:31-39
2. Kumar S N, Fred A L, Subramanian M, Haridhas A K, Varghese P S. A voyage on medical image segmentation algorithms. *Biomedical Research*. 10.4066/biomedicalresearch. 2018; 29:75-87.
3. Wallner J, Schwaiger M, Hohegger K, Gsaxner C, Zemann W, Egger J. A review on multiplatform evaluations of semi-automatic open-source based image segmentation for cranio-maxillofacial surgery. *Comput Methods Programs Biomed*. 2019; 182:105102
4. Shaheen E, Khalil W, Ezeldeen M, Van de Castele E, Sun Y, Politis C, Jacobs R. Accuracy of segmentation of tooth structures using 3 different CBCT machines. *Oral Surg Oral Med Oral Pathol Oral Radiol*. 2017;123(1):123-128.
5. Liu X, Song L, Liu S, Zhang Y. A Review of Deep-Learning-Based Medical Image Segmentation Methods. *Sustainability*. 2021; 13(3):1224.
6. Haque I R I, Neubert J. Deep learning approaches to biomedical image segmentation. *Informatics in Medicine Unlocked*, 2020,18,100297
7. Gomes AF, Brasil DM, Silva AIV, Freitas DQ, Haiter-Neto F, Groppo FC. Accuracy of ITK-SNAP software for 3D analysis of a non-regular topography structure. *Oral Radiol*. 2020;36(2):183-189.
8. Stoetzer M, Nickel F, Rana M, Lemound J, Wenzel D, von See C, et al. Advances in assessing the volume of odontogenic cysts and tumors in the mandible: a retrospective clinical trial. *Head Face Med*. 2013; 20:9:14.
9. O'Brien W.J. *Dental Materials and Their Selection*. 3rd Edition, Quintessence Publishing Co. Inc., Chicago. 2002 pp 323.
10. Ahlowalia MS, Patel S, Anwar HM, Cama G, Austin RS, Wilson R, et al. Accuracy of CBCT for volumetric measurement of simulated periapical lesions. *Int Endod J*. 2013; 46:538–546.
11. Weissheimer A, Menezes LM, Sameshima GT, Enciso R, Pham J, Grauer D. Imaging software accuracy for 3-dimensional analysis of the upper airway. *Am J Orthod Dentofacial Orthop* 2012;142: 801-13
12. Vallaey K, Kacem A, Legoux H, Le Tenier M, Hamitouche C, Arbab-Chirani R. 3D dento-maxillary osteolytic lesion and active contour segmentation pilot study in CBCT: semi-automatic vs manual methods. *Dentomaxillofac Radiol*. 2015;44(8):20150079.
13. Lo Giudice A, Ronsivalle V, Gastaldi G, Leonardi R. Assessment of the accuracy of imaging software for 3D rendering of the upper airway, usable in orthodontic and craniofacial clinical settings. *Prog Orthod*. 2022; 23, 22.
14. Park CW, Kim JH, Seo YK, Lee SR, Kang JH, Oh SH, Kim GT, Choi YS, Hwang EH. Volumetric accuracy of cone-beam computed tomography. *Imaging Sci Dent*. 2017;47(3):165-174.